

Thermodynamical string fragmentation and string density effects in jets

Róbert Vértési

*HUN-REN Wigner Research Centre for Physics
 DF13841 Konkoly-Thege Miklós út 29-33,
 1121 Budapest, Hungary*

Antonio Ortiz*

*Instituto de Ciencias Nucleares, UNAM
 Circuito exterior s/n Ciudad Universitaria,
 04510 Mexico City, Mexico
 (Dated: July 23, 2025)*

It has been proposed to search for thermal and collective properties arising from parton-fragmentation processes by examining high jet charged-constituent multiplicities ($N_{j, \text{ch}}$) in proton-proton (pp) collisions. This proposal was initially tested using the PYTHIA 8 event generator with the Monash tune, which incorporates multiparton interactions (MPI) and the MPI-based colour reconnection (CR) model. These studies did not reveal any conclusive evidence for the presence of radial flow. In this paper, we expand upon the proposed Monte Carlo study by eliminating selection biases associated with triggering on charged particle multiplicities. Furthermore, MPI are disabled to focus exclusively on jet fragments. We analyse pp collisions at $\sqrt{s}=13$ TeV simulated with PYTHIA 8, exploring different implementations of the generator: thermodynamical string fragmentation and the standard Lund fragmentation model. The impact of colour-string junctions was also explored. Surprisingly, the thermodynamical string fragmentation together with the close-packing of strings mechanism predicts a hint of baryon enhancement in jets. Additionally, the light-flavor baryon-to-meson ratios as a function of j_T exhibit similarities across all PYTHIA 8 implementations, and hint at radial flow-like effects. In contrast, the ratio of heavy-flavor hadrons (Λ_c^+/D^0) at low j_T as a function of $N_{j, \text{ch}}$ shows a trend similar to that observed as a function of charged-particle multiplicity in minimum-bias data, suggesting that colour-string junctions may play a crucial role in heavy baryon production in jets. The same mechanism also predicts a j_T -integrated Λ_c^+/D^0 ratio that increases with increasing $N_{j, \text{ch}}$. Interestingly, for the lowest $N_{j, \text{ch}}$ value, such a ratio is consistent with the e^+e^- limit, suggesting that jet multiplicity is a potential way to explore more dilute systems covering the multiplicity gap between e^+e^- and pp collisions.

I. INTRODUCTION

The heavy-ion collider experiments at the Relativistic Heavy Ion Collider (RHIC) at BNL and the Large Hadron Collider (LHC) at CERN aim to study dense QCD systems, where a new form of matter, the strongly-interacting quark-gluon plasma (QGP) is created. One major discovery of the LHC era is the observation of QGP-like effects in small-collision systems (pp and p-Pb collisions). The origin of the new phenomena has remained an open question for the past decade. In heavy-ion collisions, signatures such as collectivity and strangeness enhancement have been attributed to the formation of QGP [1–3]. On the one hand, IP-Glasma calculations indicate that the energy density, averaged over the transverse area, can reach around $70 \text{ GeV}/\text{fm}^3$ in pp collisions for charged particle multiplicity densities above 100 [4]. Lattice QCD calculations suggest that this condition is sufficient for QGP formation in pp collisions. However, no signatures of jet quenching have been observed so far [5, 6]. Moreover, long-range angular correlations have been observed even in very dilute systems

like low-multiplicity pp collisions [7], photonuclear ultra-peripheral Pb-Pb collisions [8], and probably in jets [9]. Although hydrodynamics has been applied to explain the pp and p-Pb data, some theoretical works suggest that it should not be applicable in small-collisions systems [10]. This opens the door to alternative approaches, such as colour strings, which have successfully described some aspects of pp and p-Pb data [11–14].

The exploration of diluted QCD systems has continued over the last years. Recently, in Ref. [15] authors postulate that a strongly-interacting QGP-like system can originate from a fast parton (quark or gluon) as it fragments and propagates through the QCD vacuum. Due to the intrinsic QCD coupling strength, the colour fields of the fast parton in the vacuum can produce a large number of secondary partons. These secondary partons can then interact and develop a collective expansion, which is transverse to the trajectory of the parent parton, and extends over a finite space-time volume. The idea is somewhat similar to a Monte Carlo (MC) study that showed that PYTHIA produces radial flow-like effects in dense partonic systems originating from multiparton interactions (MPI) due to string interactions via colour reconnection (CR) [16]. Since, in the standard colour reconnection schemes implemented in PYTHIA, CR effects are suppressed in jets, no radial flow-like effects and

* antonio.ortiz@nucleares.unam.mx

strangeness enhancement were reported in Ref. [15].

Inspired by Ref. [15], the CMS collaboration reported a new measurement from pp collision data with high jet charged-constituents multiplicities ($N_{j, \text{ch}}$) [9]. They studied two-particle correlations among the charged particle jet constituents as functions of the azimuthal angle and pseudorapidity separations ($\Delta\varphi^*$, $\Delta\eta^*$) in the jet coordinate frame, where η^* and φ^* are defined relative to the direction of the jet axis. The azimuthal correlation was analysed as a function of $N_{j, \text{ch}}$. For low $N_{j, \text{ch}}$ values, the long-range elliptic anisotropic harmonic, v_2^* , decreases with $N_{j, \text{ch}}$, a characteristic reproduced by models like PYTHIA 8. However, an intriguing rising trend for v_2^* is observed at $N_{j, \text{ch}} > 80$, hinting at a possible onset of collective behaviour, which is not reproduced by the MC generators that were tested. The observation is interesting and deserves further study, particularly for high- $N_{j, \text{ch}}$ values.

This paper reports on the search for baryon enhancement and radial flow-like effects in jets. A crucial difference from Ref. [15] is that the bias due to the multiplicity selection based on charged particles is removed by reporting the hyperon-to- K_S^0 ratios instead of the hyperon-to-charged-pion ratios. In addition, the baryon-to-meson ratio in the charm sector is also investigated. For both studies, various models are tested, including the standard Lund string fragmentation model with different colour-reconnection implementations, as well as the thermodynamical string fragmentation model [17]. The current work is relevant for understanding QGP-like effects observed in small systems, and may also help resolve a long-standing puzzle, that in elementary e^+e^- collisions the yields of various hadron species can be well described by a thermal statistical model [18].

The paper is organised as follows. The PYTHIA MC event generator and the different models used in this work are introduced in section II. Section III presents the methodology, as well as comparisons between models and data. Section IV presents the results and discussion. Finally, results are summarised in section V.

II. PYTHIA MODELS

The results presented in this paper are obtained from PYTHIA simulations [19] (version 8.309), which incorporate the Lund string fragmentation model [20]. The Monash tune has been obtained from fits to early LHC data; therefore, it successfully describes several observables at LHC energies. The model incorporates MPI and CR, which are crucial for reproducing the multiplicity distributions as well as the correlation between the average transverse momentum (p_T) and the charged-particle multiplicity [21]. Since the discovery of radial flow-like effects due to the CR mechanism, more advanced CR models have been built [22]. The most common CR models use the leading colour (LC) approximation to calculate the colour flow on an event-by-event basis; the partonic

final states result from colour-connecting a quark to another single and unique parton in the event. In the model, gluons carry both a colour and an anticolour charge, and therefore they are connected to two other partons. The LC approximation is used in the MPI-based colour reconnection model implemented in the Monash tune. In this scheme, each MPI-scattering system is viewed as separate and distinct from all other systems in colour space. The colour flow of two such systems can be fused, and if so, the partons of the lower- p_T system are added to the strings defined by the higher- p_T system to minimise the total string length. In this paper we also consider colour reconnection modes beyond leading colour approximation (CR-BLC). The QCD-scheme CR, which considers the minimisation of the string length and the colour rules from QCD, constructs all pairs of dipoles that are allowed to reconnect by QCD-colour rules and switches if the new pair has a lower string length. Junctions can also be directly produced from three, and in some special cases, four dipoles. Here, the multiplet structure of SU(3) is combined with a minimisation of the string potential energy, to decide between which partons strings should form, allowing also for “baryonic” configurations. One would expect that MPI increases the number of possible subleading connections. [23]. It is worth mentioning that in the traditional approach, also implemented in the MPI-based CR scheme, CR effects are negligible in jets and are enhanced in active MPI environments. Although the QCD-based CR model implemented in PYTHIA reproduces basic observables well, further tunes have been developed considering different time-dilation constraints [22]. The CR-BLC mode 2, which requires strict causality between dipoles, is proven to reproduce the features seen in the heavy-flavor baryonic sector [24–26].

The models described above are based on the standard Lund string fragmentation, where a tunneling mechanism for string breakups results in a Gaussian suppression of the production of heavier quarks and diquarks, with a further suppression based on the hadronic spin state. In the thermodynamical string fragmentation [17], the Gaussian suppression in mass and p_T is replaced by an exponential suppression. The experimental motivation comes from fixed-target and ISR data, which show that the inclusive p_T distributions are well described by an exponential function, $\exp(-Bp_T)$ with $B \approx 6 \text{ GeV}^{-1}$. The model exhibits reasonable agreement with LHC data for observables such as the p_T distributions of unidentified charged hadrons, the average transverse momentum as a function of the hadron mass, and hyperon-to-pion ratios as a function of multiplicity. The set of parameters for thermodynamical-string fragmentation includes the modification of string tension due to the local string density [17]. This mechanism is named close packing. In minimum-bias pp collisions an effective string density is introduced for low p_T , while jet fragmentation occurs outside the close-packing string region and is left unaffected. This mechanism changes the flavour composi-

tion at high multiplicities. In this paper, we explore the potential impact of these new implementations in high-string density environments such as high jet-charged-constituent multiplicities.

The relevant parameters are summarized in Table I. In the following, the model named as **Monash CR-QCD** is the Monash tune with the QCD-based CR parameters, which is essentially Monash tune including colour-string junctions. Variations of Monash tune including thermodynamical-string fragmentation with MPI-based and QCD-based CR models are termed **Thermodyn.** and **Thermodyn. CR-QCD** models, respectively. Finally, the model **CR-BLC mode2** is a tuned version of PYTHIA 8 including colour-string junctions.

III. ANALYSIS METHOD

Before discussing the observables in the jet frame, Fig. 1 shows the p_T spectra of various particle species, comparing the model predictions described above with the minimum-bias pp ALICE data [27, 28]. Note that there are certain differences between simulations and data in handling charm hadrons: in the current study, the feed-down components into charm hadrons have not been excluded, and a pseudorapidity cut $|\eta| < 1$ was used instead of a rapidity cut $|y| < 0.5$ on the charm hadrons, $|\eta| < 0.5$ on their decay products as considered in Ref. [28]. Overall, all models yield similar results for unidentified charged particles, charged pions, kaons and (anti)protons. The spectral shapes are well reproduced by models both at low and high p_T . For heavier hadrons, the models deviate from each other. The Λ - p_T spectrum is better described by the Monash CR-QCD and CR-BLC mode2 models suggesting the important role of colour-string junctions. The thermodynamical-string fragmentation models predict a slightly lower yield, probably because the model has not been tuned to data. However, the Ξ^\pm and Ω^\pm baryon- p_T spectra are best described by the simulations, which consider thermodynamical-string fragmentation. Although the best agreement is observed for Ω^\pm , the other models significantly underpredict particle yield within the measured p_T range (1–4 GeV/c). It is worth noting that the Thermodyn. model matches the data better than the Thermodyn. CR-QCD model, which overpredicts the yield. For the heavy-flavour sector (D^0 meson and Λ_c^\pm), the best description is provided by models incorporating colour-string junctions (Monash CR-QCD, CR-BLC mode2 and Thermodyn. CR-QCD), which promote the baryon formation particularly in the charm sector.

For jet observables, the simulations were performed with the HardQCD setting and a phase-space cut of $\hat{p}_T > 550$ GeV/c. Jets were clustered using the anti- k_T algorithm [29] with the energy recombination scheme and a resolution parameter $R = 0.8$. Jets with charged-jet transverse momenta $550 < p_T^{\text{jet}} < 1000$ GeV/c were

used. The mean \hat{p}_T is about 744 GeV/c. To correct for the bias introduced by the phase-space cut, we applied a p_T^{jet} -dependent correction, which is in the order of 15% at $p_T^{\text{jet}} = 550$ GeV and vanishes towards higher momenta. We made sure through a cross-check with $\hat{p}_T > 250$ GeV/c that the phase-space cut has negligible effect on our observables. Also note that we applied a selection on p_T^{jet} corresponding to charged jets. Applying full jet transverse-momentum selection similarly to Ref. [9] results in a momentum shift, which affects the reach in $N_{j,\text{ch}}$ but the baryon-to-meson ratios are largely unaffected. Since we focus on jet observables, we disabled multiparton interactions to avoid background from the underlying event unrelated to the jets. In the analysis, we use the jet frame [15] to define the kinematics of jet constituents as $\mathbf{p}^* = (j_T, \eta^*, \varphi^*)$, where j_T is the momentum component perpendicular to the jet axis, and η^* - φ^* were already defined.

IV. RESULTS AND DISCUSSION

Figure 2 (left) shows the $N_{j,\text{ch}}$ distributions for various model settings. The jet multiplicities show slight variations depending on the colour-reconnection scheme and also differ slightly in the case of thermodynamical string fragmentation. In particular, the high- $N_{j,\text{ch}}$ tail is slightly reduced in the Monash CR-QCD, CR-BLC mode2, and Thermodyn. CR-QCD models compared to Monash. The η^* distributions, shown in the right panel, appear to be independent of the model settings used. In the jet coordinate system, low- η^* values correspond to charged particles that are separated from the jet axis by large angles, whereas the high- η^* values are associated with particles at small angles relative to the jet direction. All curves exhibit a steep rise up to $\eta^* \approx 0.86$, which is related to the choice of the jet resolution parameter ($R = 0.8$).

To reveal the dynamics of various constituents within a jet, their production can be analysed using kinematic variables in the co-moving frame. Figure 3 shows different baryon-to-meson ratios as a function of j_T , for different models, in several $N_{j,\text{ch}}$ classes.

Before discussing the particle ratios, it is important to note that the models predict larger emission angles and j_T values for high jet charged-constituent multiplicities compared to the inclusive and low- $N_{j,\text{ch}}$ event classes. Conversely, lower emission angles (and lower j_T values) are expected for low $N_{j,\text{ch}}$ pp collisions. This effect is due to a correlation between jet-charged-constituent multiplicity and the flavour of its initiating parton, with high- $N_{j,\text{ch}}$ values predominantly associated to gluon-initiated jets and low- $N_{j,\text{ch}}$ values to quark-initiated jets [15].

In the light-flavour sector, all models (Monash, Monash CR-QCD, CR-BLC mode2 and Thermodyn. CR-QCD) exhibit some common features in baryon-to-meson ratios. For $j_T > 5$ GeV/c, the proton-to-pion and the Λ^0 -to- K_S^0 ratios are grouped into low- $N_{j,\text{ch}}$ and high-

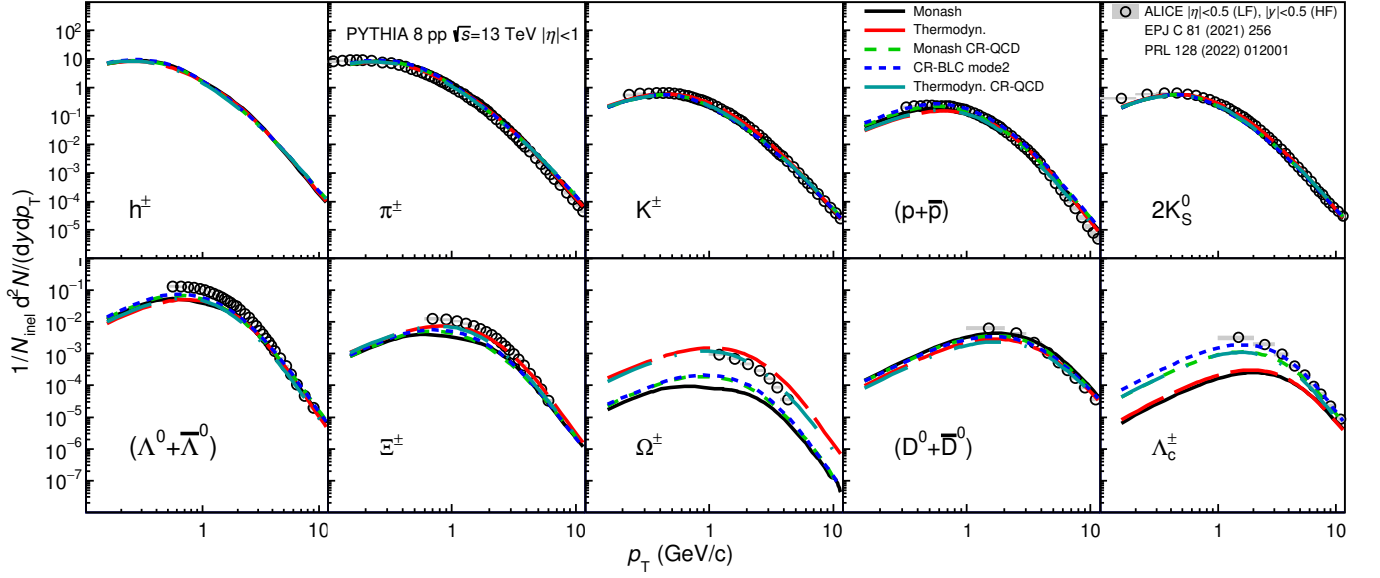


FIG. 1. Midrapidity transverse momentum spectra of identified hadrons in pp collisions at $\sqrt{s} = 13$ TeV. Data are compared with different model predictions.

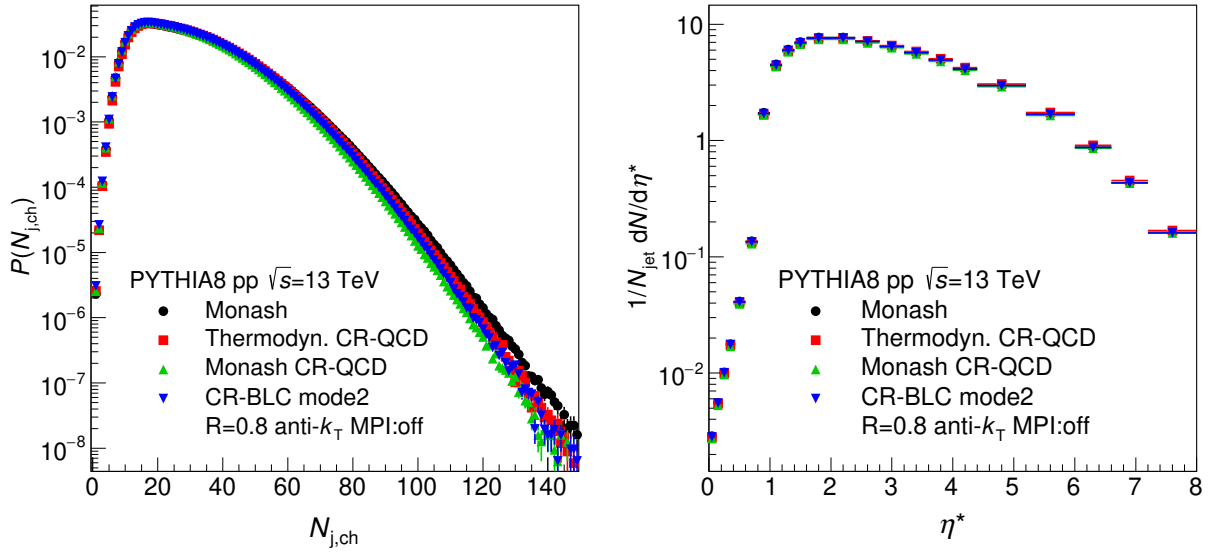


FIG. 2. Jet charged-constituent multiplicity (left) and η^* (right) distributions for different model settings. Results for pp collisions at $\sqrt{s} = 13$ TeV are displayed. MPI is off in all cases.

$N_{j,ch}$ ranges, with the ratios for $0 < N_{j,ch} < 20$ and $20 < N_{j,ch} < 40$ being lower than those for the higher $N_{j,ch}$ intervals: 40-60, 60-80, 80-100, 100-120. This grouping may reflect the flavour of the initiating parton. Looking at the details, the ratios are slightly multiplicity dependent, as they increase with increasing $N_{j,ch}$. On the other hand, for lower j_T values ($j_T < 5$ GeV/c) the multiplicity dependence is stronger: the ratios are depleted from the low- to high- $N_{j,ch}$ classes. For all $N_{j,ch}$ classes, the ratios show a bump structure which shifts towards higher j_T values with increasing $N_{j,ch}$. The effect

is similar to that observed in p_T in the standard multiplicity analysis, where it is attributed to radial flow-like effects [30]. All these features, except for the multiplicity grouping, are also present in the Ξ^\pm -to- K_S^0 particle ratio. The presence of the bump is not obvious in the case of the multistrange Ω^\pm -to- K_S^0 ratio, except in the Thermodyn. CR-QCD model, where a strong enhancement of Ω^\pm is observed compared to other models. However, this enhancement is less pronounced in high- $N_{j,ch}$ pp collisions at low- j_T , and only gets stronger with $N_{j,ch}$ towards mid- and high- j_T values.

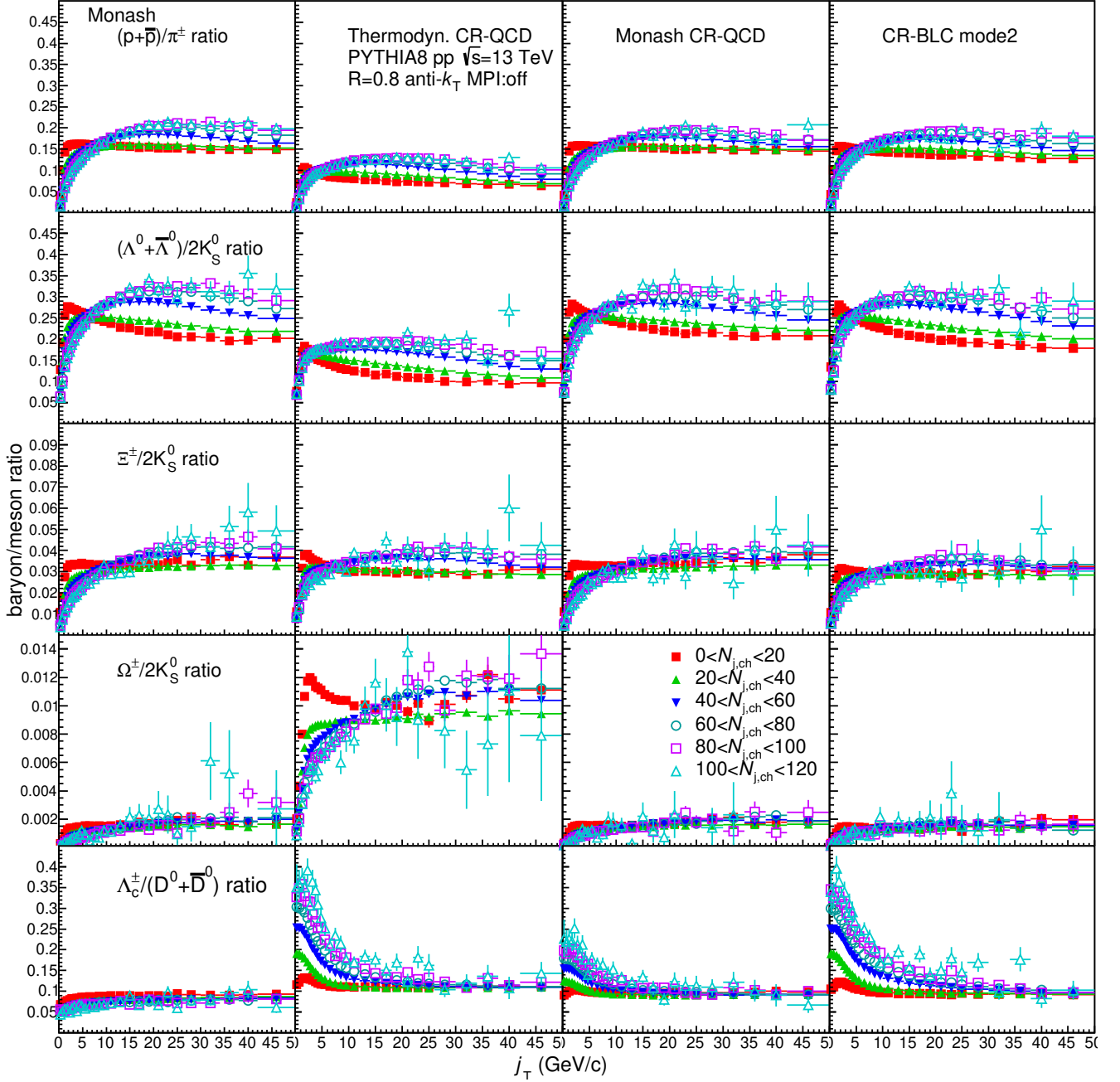


FIG. 3. Baryon-to-meson ratios as a function of j_T for different jet charged-constituent multiplicity intervals. Results are shown for pp collisions at $\sqrt{s} = 13$ TeV, simulated with different PYTHIA settings. MPI is off in all cases.

For the heavy-flavour particle ratio, Λ_c/D^0 , no enhancement is seen with the Monash model at low j_T . However, Monash CR-QCD shows a clear Λ_c^+/D^0 enhancement at lower j_T values, which is more pronounced with increasing $N_{j, \text{ch}}$. This phenomenon is even stronger for the CR-BLC mode2 and Thermodyn. CR-QCD models. Keeping in mind that string junctions have an impact on the baryon-to-meson ratio at low p_T [26, 31–33], the observed patterns in jets could be due to colour-string junctions. One should remember that the Λ_c^+/D^0 ra-

tios as a function of p_T are well described by PYTHIA 8 including colour-string junctions. A similar feature to the $N_{j, \text{ch}}$ -dependent excess at low j_T values has also been seen in CR-BLC simulations toward higher p_T values, where the Λ_c^+/D^0 ratios were found to depend on the jet activity [34]. Regarding the CR-BLC mode2 and Thermodyn. CR-QCD models, it is also interesting to note that for the highest $N_{j, \text{ch}}$ class, the maximum value for Λ_c^+/D^0 is approximately 0.35, similar to the value reported for the lowest inclusive multiplicity class

in Ref. [24] suggesting that intra-jet multiplicities is a promising venue to explore the multiplicity gap between e^+e^- to pp collisions. This conclusion is further supported by the fact that for the lowest $N_{j,\text{ch}}$ class the ratios are nearly flat and consistent with the corresponding ratios measured in e^+e^- collisions at LEP, which was found to be $0.113 \pm 0.013(\text{stat}) \pm 0.006(\text{syst})$ [35]. Note that in the low- $N_{j,\text{ch}}$ limit, one would expect the jet sample to be dominated by quark-initiated jets. It is also important to note that while there are more recent models for colour reconnection with colour junctions [36, 37], there is no significant difference of the Λ_c/D^0 predictions provided by CR-BLC and these new models. Therefore, we stick to CR-BLC, which is widely used by the community.

Figure 4 shows the baryon-to-meson ratios integrated over j_T , as a function of $N_{j,\text{ch}}$. A notable feature is that the standard Lund string fragmentation (Monash, Monash CR-QCD, and CR-BLC mode2 models) predicts higher $(p + \bar{p})/(\pi^+ + \pi^-)$ and Λ^0/K_s^0 and lower Ξ^\pm/K_s^0 and Ω^\pm/K_s^0 ratios than the Thermodyn. CR-QCD model in the full $N_{j,\text{ch}}$ range. The standard Lund model predicts either decreasing or nearly constant particle ratios with increasing $N_{j,\text{ch}}$. In contrast, the Thermodyn. CR-QCD model shows a continuous increase in $(p + \bar{p})/(\pi^+ + \pi^-)$, Λ^0/K_s^0 , and Ξ^\pm/K_s^0 with increasing $N_{j,\text{ch}}$. This indicates a kind of baryon enhancement for jet constituents. However, for Ω^\pm/K_s^0 , the Thermodyn. CR-QCD model predicts a ratio that is 5 times higher than that predicted by other models, and a decreasing trend with increasing jet multiplicity, which aligns with the findings reported by authors of the thermodynamical string fragmentation model [17]. In this model, heavier hadrons tend to be produced at large p_T values (in the jet), which might explain the difference from the standard Lund fragmentation model. The same paper notes that the Ω yield normalised to the charged-pion yield decreases with growing multiplicity, likely due to phase-space constraints. Looking at Table I, one notices the parameter `StringFlav:BtoMratio` in the Thermodyn. CR-QCD model, which controls the relative rate of baryon-to-meson production. We changed this parameter and verified that the multiplicity dependence of the baryon-to-meson ratios were not affected by such a variation.

Finally, the Λ_c^+/D^0 ratio shows an increasing trend with $N_{j,\text{ch}}$ for the models including colour-string junctions (Monash CR-QCD, CR-BLC mode2 and Thermodyn. CR-QCD models), while there is an opposite trend for Monash. It is worth mentioning that ALICE data exhibit a p_T -integrated Λ_c^+/D^0 ratio that is multiplicity independent. Thus, intra-jet studies in the data could be highly valuable for testing different baryon production models and contribute to a deeper understanding of the QGP-like effects observed in small systems.

It is worth noting that the Thermodyn. CR-QCD model produces baryon enhancement relative to mesons (except for the Ω baryon), and also predicts a Λ_c^+/D^0 ratio that starts from ≈ 0.11 (close to the e^+e^- limit) followed by an increase with increasing $N_{j,\text{ch}}$. Then the

question is whether these effects have to do with the CR model and/or the close-packing mechanism. The plot on the right-hand side of Fig. 4 shows the baryon-to-meson ratios integrated over j_T , as a function of $N_{j,\text{ch}}$ for the Thermodyn. model, where no colour-string junctions are considered. Simulations including the close-packing mechanism exhibit baryon enhancement relative to mesons for $(p + \bar{p})/(\pi^+ + \pi^-)$, Λ^0/K_s^0 , Ξ^\pm/K_s^0 , and Ω^\pm/K_s^0 particle ratios. On the contrary, the enhancement is not observed when the close-packing mechanism is disabled. Therefore, such an enhancement in the light and strange baryon sector is due to thermodynamical string fragmentation and the close-packing mechanism. In contrast, looking at the heavy flavour sector, the Λ_c^+/D^0 ratio is nearly flat in Thermodyn. model suggesting the importance of colour-string junctions in the production of heavy baryons.

V. CONCLUSIONS

This paper reports on intra-jet identified-hadron production as a function of the jet charged-constituent multiplicity ($N_{j,\text{ch}}$) in pp collisions at $\sqrt{s} = 13$ TeV simulated with PYTHIA 8. The jet frame is used to define the kinematics of jet constituents: j_T is the momentum component perpendicular to the jet axis, η^* and φ^* are the pseudorapidity and azimuthal angle coordinates with respect to the jet axis, respectively. The multiparton interaction mechanism is turned off. Given that only charged particles are considered to calculate $N_{j,\text{ch}}$, the light-flavour baryon yields are normalised to the K_s^0 yield. Thus, no bias in the neutral-to-charged particle ratio affects the results.

The pp collisions are simulated using the Monash tune, which implements the MPI-based CR model. The effect of colour-string junctions is studied by means of a comparison between the Monash tune and the so-called Monash CR-QCD model. Other studies were performed that included variations of the Monash tune, including thermodynamical string fragmentation with MPI-based and QCD-based CR models named Thermodyn. and Thermodyn. CR-QCD models, respectively. Finally, the model CR-BLC mode2, which is a tuned version of PYTHIA 8 including colour-string junctions, was also included in the study.

- The $N_{j,\text{ch}}$ and η^* distributions are only slightly or not affected by the choice of the PYTHIA settings.
- For all PYTHIA models the proton-to-pion and the Λ^0 -to- K_s^0 ratios show low-high multiplicity grouping trend for $j_T > 5$ GeV/c, possibly reflecting the flavour of the jet-initiating parton. The ratios show a bump structure that shifts towards higher j_T values with increasing $N_{j,\text{ch}}$. This effect is reminiscent of the radial flow-like effects observed in the p_T spectra as a function of the inclusive charged particle multiplicity. These features, except the mul-

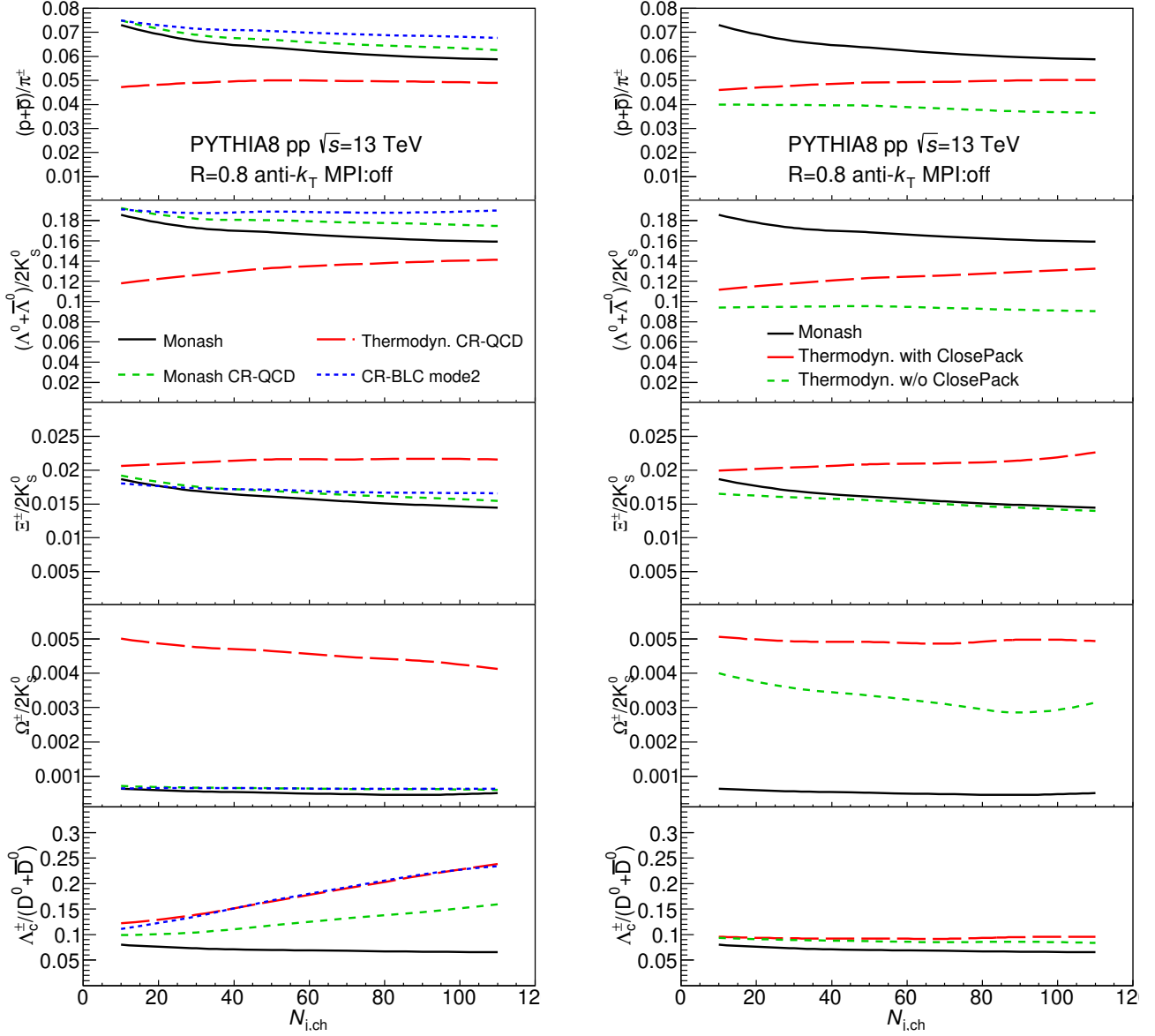


FIG. 4. Baryon-to-meson ratios as a function of the jet charged-constituents multiplicity. Results for pp collisions at $\sqrt{s} = 13$ TeV simulated with different PYTHIA settings. The different colour-reconnection schemes (left) and the effect of thermodynamical string fragmentation with and without close packing (right) are compared to the Monash tune. MPI is off in all cases.

tiplicity grouping, are also seen in the Ξ^\pm -to- K_S^0 particle ratios. The presence of the bump is not obvious in the case of the multistrange Ω^\pm -to- K_S^0 ratio, except in the thermodynamical string fragmentation model, where a strong enhancement of Ω^\pm is observed compared to other models.

- Λ_c^+/D^0 as a function of j_T is little or not multiplicity dependent for Monash tune. However, colour-string junctions (Monash CR-QCD) produce an increase in the Λ_c^+/D^0 ratio at low j_T with increasing $N_{j,ch}$. The effect gets enhanced for the tune CR-BLC mode2, which also includes colour-string

junctions. The size of the effects for the later model is consistent with that produced by Thermodyn. CR-QCD model. This effect is similar to the multiplicity-dependent Λ_c^+/D^0 as a function p_T reported by ALICE. For the lowest $N_{j,ch}$ class, the ratio is nearly flat and is consistent with the corresponding ratios measured in e^+e^- collisions at LEP.

- Regarding the j_T -integrated baryon-to-meson particle ratios for the light-flavoured sector, the Thermodyn. model with string density effects (close-packing mechanism) produces ratios that increase

with $N_{j,\text{ch}}$. On the other hand, the Λ_c^+/D^0 ratio shows an increasing trend with $N_{j,\text{ch}}$ for models including colour-string junctions. The ratio departs from ≈ 0.11 (consistent with e^+e^- limit) and increases with $N_{j,\text{ch}}$. These findings encourage intra-jet studies to be relevant in covering the multiplicity gap between e^+e^- and pp collisions.

The results presented in this paper provide new observables that can be used to test thermodynamics-inspired fragmentation models, as well as the role of colour-string junctions in the heavy-flavoured hadron production from

small to large systems.

ACKNOWLEDGEMENTS

Authors acknowledge the useful discussions with Torbjörn Sjöstrand. R. V. acknowledges the support by the Hungarian National Research, Development and Innovation Office (NKFIH) under the contract numbers OTKA FK131979 and 2021-4.1.2-NEMZ_KI-2022-00034. A. O. acknowledges the support by DGAPA-UNAM under the grants PAPIIT No. IG100524 and PAPIME No. PE100124.

-
- [1] W. Busza, K. Rajagopal, and W. van der Schee, Heavy Ion Collisions: The Big Picture, and the Big Questions, *Ann. Rev. Nucl. Part. Sci.* **68**, 339 (2018), arXiv:1802.04801 [hep-ph].
 - [2] R. Bala, I. Bautista, J. Bielcikova, and A. Ortiz, Heavy-ion physics at the LHC: Review of Run I results, *Int. J. Mod. Phys. E* **25**, 1642006 (2016), arXiv:1605.03939 [hep-ex].
 - [3] S. Acharya *et al.* (ALICE), The ALICE experiment – A journey through QCD, (2022), arXiv:2211.04384 [nucl-ex].
 - [4] S. Acharya *et al.* (ALICE), Future high-energy pp programme with ALICE, ALICE-PUBLIC-2020-005 (2020).
 - [5] S. Acharya *et al.* (ALICE), Study of charged particle production at high p_T using event topology in pp, p–Pb and Pb–Pb collisions at $\sqrt{s_{NN}} = 5.02$ TeV, *Phys. Lett. B* **843**, 137649 (2023), arXiv:2204.10157 [nucl-ex].
 - [6] S. Acharya *et al.* (ALICE), Search for jet quenching effects in high-multiplicity pp collisions at $\sqrt{s} = 13$ TeV via di-jet acoplanarity, *JHEP* **05**, 229, arXiv:2309.03788 [hep-ex].
 - [7] S. Acharya *et al.* (ALICE), Emergence of long-range angular correlations in low-multiplicity proton-proton Collisions, *Phys. Rev. Lett.* **132**, 172302 (2024), arXiv:2311.14357 [nucl-ex].
 - [8] G. Aad *et al.* (ATLAS), Two-particle azimuthal correlations in photonuclear ultraperipheral Pb–Pb collisions at $\sqrt{s_{NN}} = 5.02$ TeV with ATLAS, *Phys. Rev. C* **104**, 014903 (2021), arXiv:2101.10771 [nucl-ex].
 - [9] A. Hayrapetyan *et al.* (CMS), Observation of Enhanced Long-Range Elliptic Anisotropies Inside High-Multiplicity Jets in pp Collisions at $\sqrt{s}=13$ TeV, *Phys. Rev. Lett.* **133**, 142301 (2024), arXiv:2312.17103 [hep-ex].
 - [10] C. Werthmann, V. E. Ambrus, and S. Schlichting, System size dependence of pre-equilibrium and applicability of hydrodynamics in heavy-ion collisions, *PoS Hard-Probes2023*, 048 (2024), arXiv:2307.08306 [hep-ph].
 - [11] D. d’Enterria, G. K. Eyyubova, V. L. Korotkikh, I. P. Lokhtin, S. V. Petrushanko, L. I. Sarycheva, and A. M. Snigirev, Estimates of hadron azimuthal anisotropy from multiparton interactions in proton-proton collisions at $\sqrt{s} = 14$ TeV, *Eur. Phys. J. C* **66**, 173 (2010), arXiv:0910.3029 [hep-ph].
 - [12] C. Bierlich, G. Gustafson, L. Lönnblad, and A. Tarasov, Effects of overlapping strings in pp collisions, *JHEP* **03**, 148, arXiv:1412.6259 [hep-ph].
 - [13] C. Bierlich, G. Gustafson, L. Lönnblad, and H. Shah, The Angantyr model for heavy-ion collisions in PYTHIA 8, *JHEP* **10**, 134, arXiv:1806.10820 [hep-ph].
 - [14] A. Ortiz, G. Bencedi, and F. Fan, Flattenicity as centrality estimator in p–Pb collisions simulated with PYTHIA/Angantyr, *J. Phys. G* **51**, 125003 (2024), arXiv:2407.07724 [nucl-ex].
 - [15] A. Baty, P. Gardner, and W. Li, Novel observables for exploring QCD collective evolution and quantum entanglement within individual jets, *Phys. Rev. C* **107**, 064908 (2023), arXiv:2104.11735 [hep-ph].
 - [16] A. Ortiz, P. Christiansen, E. Cuautle, I. Maldonado, and G. Pać, Color reconnection and flowlike patterns in pp collisions, *Phys. Rev. Lett.* **111**, 042001 (2013), arXiv:1303.6326 [hep-ph].
 - [17] N. Fischer and T. Sjöstrand, Thermodynamical string fragmentation, *JHEP* **01**, 140, arXiv:1610.09818 [hep-ph].
 - [18] F. Becattini, A Thermodynamical model of hadron production in e^+e^- collisions, in *25th International Symposium on Multiparticle Dynamics* (1995) pp. 480–490, arXiv:hep-ph/9511235.
 - [19] T. Sjöstrand, S. Ask, J. R. Christiansen, R. Corke, N. Desai, P. Ilten, S. Mrenna, S. Prestel, C. O. Rasmussen, and P. Z. Skands, An introduction to PYTHIA 8.2, *Comput. Phys. Commun.* **191**, 159 (2015), arXiv:1410.3012 [hep-ph].
 - [20] B. Andersson, G. Gustafson, G. Ingelman, and T. Sjöstrand, Parton fragmentation and string dynamics, *Phys. Rept.* **97**, 31 (1983).
 - [21] P. Skands, S. Carrazza, and J. Rojo, Tuning PYTHIA 8.1: the Monash 2013 Tune, *Eur. Phys. J. C* **74**, 3024 (2014), arXiv:1404.5630 [hep-ph].
 - [22] J. R. Christiansen and P. Z. Skands, String formation beyond leading colour, *JHEP* **08**, 003, arXiv:1505.01681 [hep-ph].
 - [23] C. Bierlich, G. Gustafson, and L. Lönnblad, A shoving model for collectivity in hadronic collisions, (2016), arXiv:1612.05132 [hep-ph].
 - [24] S. Acharya *et al.* (ALICE), Observation of a multiplicity dependence in the p_T -differential charm baryon-to-meson ratios in proton-proton collisions at $\sqrt{s} = 13$ TeV, *Phys.*

PYTHIA 8 Parameter	Monash	Monash CR-QCD	CR-BLC (mode 2)	Thermodyn.	Thermodyn. CR-QCD
StringPT:sigma	0.335	0.335	0.335	0.335	0.335
StringPT:closePacking	off	off	off	on	on
StringPT:thermalModel	off	off	off	on	on
StringPT:temperature				0.21	0.21
StringPT:expNSP				0.13	0.13
StringZ:aLund	0.68	0.68	0.36	0.68	0.68
StringZ:bLund	0.98	0.98	0.56	0.98	0.68
StringFlav:BtoMratio				0.357	0.357
StringFlav:StrangeSuppression				0.357	0.357
StringFlav:probQQtoQ	0.081	0.081	0.078		
StringFlav:ProbStoUD	0.217	0.217	0.2		
StringFlav:probQQ1toQQ0join	0.5	0.5	0.0275	0.5	0.5
	0.7	0.7	0.0275	0.7	0.7
	0.9	0.9	0.0275	0.9	0.9
	1.0	1.0	0.0275	1.0	1.0
BeamRemnants:remnantMode	0	1	1	0	1
BeamRemnants:saturation		5	5		5
ColourReconnection:mode	0	1	1	0	1
ColourReconnection:allowDoubleJunRem	on	on	off	on	on
ColourReconnection:m0	0.3	0.3	0.3	0.3	0.3
ColourReconnection:allowJunctions		on	on		on
ColourReconnection:junctionCorrection		1.20	1.20		1.20
ColourReconnection:timeDilationMode		2	2		2
ColourReconnection:timeDilationPar		0.18	0.18		0.18

TABLE I. List of the relevant parameters of the different PYTHIA 8 settings used in the current work. Also see Refs. [17, 21, 22]

- Lett. B **829**, 137065 (2022), arXiv:2111.11948 [nucl-ex].
- [25] S. Acharya *et al.* (ALICE), Charm production and fragmentation fractions at midrapidity in pp collisions at $\sqrt{s} = 13$ TeV, JHEP **12**, 086, arXiv:2308.04877 [hep-ex].
- [26] A. M. Sirunyan *et al.* (CMS), Production of Λ_c^+ baryons in proton-proton and lead-lead collisions at $\sqrt{s_{NN}} = 5.02$ TeV, Phys. Lett. B **803**, 135328 (2020), arXiv:1906.03322 [hep-ex].
- [27] S. Acharya *et al.* (ALICE), Production of light-flavor hadrons in pp collisions at $\sqrt{s} = 7$ and $\sqrt{s} = 13$ TeV, Eur. Phys. J. C **81**, 256 (2021), arXiv:2005.11120 [nucl-ex].
- [28] S. Acharya *et al.* (ALICE), Measurement of Prompt D^0 , Λ_c^+ , and $\Sigma_c^{0,++}(2455)$ Production in Proton-Proton Collisions at $\sqrt{s} = 13$ TeV, Phys. Rev. Lett. **128**, 012001 (2022), arXiv:2106.08278 [hep-ex].
- [29] M. Cacciari, G. P. Salam, and G. Soyez, The anti- k_T jet clustering algorithm, JHEP **04**, 063, arXiv:0802.1189 [hep-ph].
- [30] S. Acharya *et al.* (ALICE), Multiplicity dependence of light-flavor hadron production in pp collisions at $\sqrt{s} = 7$ TeV, Phys. Rev. C **99**, 024906 (2019), arXiv:1807.11321 [nucl-ex].
- [31] S. Acharya *et al.* (ALICE), Λ_c^+ production in pp collisions at $\sqrt{s} = 7$ TeV and in p-Pb collisions at $\sqrt{s_{NN}} = 5.02$ TeV, JHEP **04**, 108, arXiv:1712.09581 [nucl-ex].
- [32] S. Acharya *et al.* (ALICE), Λ_c^+ production and baryon-to-meson ratios in pp and p-Pb collisions at $\sqrt{s_{NN}}=5.02$ TeV at the LHC, Phys. Rev. Lett. **127**, 202301 (2021), arXiv:2011.06078 [nucl-ex].
- [33] R. Aaij *et al.* (LHCb), Prompt Λ_c^+ production in p-Pb collisions at $\sqrt{s_{NN}} = 5.02$ TeV, JHEP **02**, 102, arXiv:1809.01404 [hep-ex].
- [34] Z. Varga and R. Vertesi, The role of the underlying event in the enhancement in high-energy pp collisions, J. Phys. G **49**, 075005 (2022), arXiv:2111.00060 [hep-ph].
- [35] L. Gladilin, Fragmentation fractions of c and b quarks into charmed hadrons at LEP, Eur. Phys. J. C **75**, 19 (2015), arXiv:1404.3888 [hep-ex].
- [36] C. Bierlich, G. Gustafson, L. Lönnblad, and H. Shah, The dynamic hadronization of charm quarks in heavy-ion collisions, Eur. Phys. J. C **84**, 231 (2024), arXiv:2309.12452 [hep-ph].
- [37] J. Altmann and P. Skands, String junctions revisited, JHEP **07**, 238, arXiv:2404.12040 [hep-ph].
- [38] A. M. Sirunyan *et al.* (CMS), Observation of enhanced long-range elliptic anisotropies inside high-multiplicity jets in pp collisions at the LHC, CMS-PAS-HIN-21-013 (2023).